

Practical Low-density Codes for PB-ToF Sensing

Alvaro Lopez Paredes, and Miguel Heredia Conde
 Center for Sensor Systems (ZESS), University of Siegen, Germany
 alvaro.lparedes@uni-siegen.de, heredia@zess.uni-siegen.de

Abstract—An indirect Pulse-based Time-of-Flight camera can be modelled as a linear sensing system in which the target’s depth is recovered from few measurements through a sensing matrix formed by a set of demodulation functions. Each demodulation function is the result of the convolution of a (0,1)-binary code and a cross-correlation function which models the entire modulation-demodulation process. In this paper, we present a practical scheme for the construction of the sensing matrix which relies on the optimization of the coherence, and is based on low-density codes. We demonstrate that our methodology eliminates the intrinsic variability of random and pseudo-random approaches, and allows for the recovery of the target’s depth in a grid much finer than the number of distinct elements in the binary codes.

I. INTRODUCTION

Time-of-Flight (ToF) systems generate a 3D representation of the surrounding space by calculating the time of the return-trip of a light signal from the sensor to the target. In indirect Pulse-based (PB)-ToF systems, as the one presented in Fig. 1 for our prototype, the target’s depth is recovered from samples of the correlation of the scene response function $[x^j]_{j=1}^n$ and a number of demodulation functions generated in the camera $[(a_i^j)]_{i=1}^m$, such that $y_i = \sum_{j=1}^n a_i^j \cdot x^j$ with $i = 1 : m$, and $m \ll n$ [1]. Retrieving \vec{x} from \vec{y} is an under-determined problem, and translates into a linearly-constrained ℓ_0 -minimization problem (1) considering the sparsity (or compressibility) of the scene response function.

$$\hat{\vec{x}} = \arg \min_{\vec{x}} \|\vec{x}\|_0, \quad \text{s.t.: } \vec{y} = \mathbf{A} \cdot \vec{x} \quad (1)$$

The demodulation function $[\vec{a}_i]_{i=1}^m$ is the result of the convolution of a (0,1)-binary code and the cross-correlation function, that models the entire modulation-demodulation process and can be approximated by a Gaussian filter with $\sigma \sim \mathcal{O}(\text{ns})$. The discrete modelling of $[\vec{a}_i]_{i=1}^m$ in a grid much finer than the one established by the (0,1)-binary codes, i.e., $n_{\text{samples}} \gg n$, allows for a much more precise localization of the target, i.e., to reach time (depth) super-resolution ($\gamma_{\text{SR}} = \frac{n_{\text{samples}}}{n} > 1$). In addition, the reduction of the number of

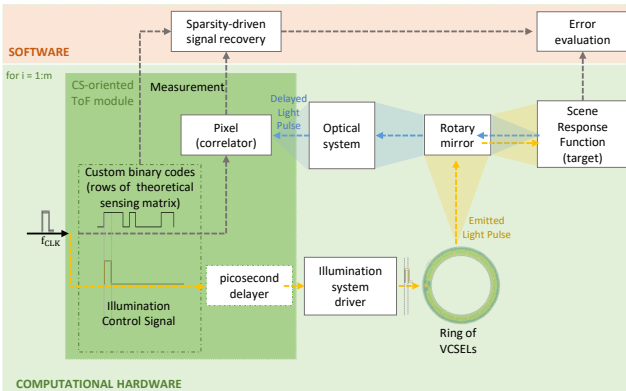


Fig. 1. Coded demodulation scheme for the PB-ToF camera designed at ZESS destined to very-wide-area applications.

measurements m becomes a key parameter to approach real-time, as the pixels require a certain amount of time $t_{\text{exp}} \sim \mathcal{O}(\text{ms})$ to gather enough light. The construction of \mathbf{A} under these premises is not an easy task, as oversampling translates into high coherence (2) ($\mu = 1$) and, therefore, to an ill-posed problem.

$$\mu = \max \left(\frac{|\vec{a}^{k^T} \cdot \vec{a}^j|}{\|\vec{a}^k\|_2 \|\vec{a}^j\|_2} \right) \quad \text{with } k \neq j \quad (2)$$

Random and Hadamard-derived (0,1)-binary codes may be used in the modulation/demodulation schemes [2], as the resulting sensing matrices ensure good recoverability properties for moderate aspect ratios ($\eta = \frac{m}{n}$), as shown in Fig. 2. However, these schemes may lead to $\mu = 1$ for $\eta \ll 1$. To solve that issue, some deterministic approaches such as the ones which make use of Low-Density Parity-Check (LDPC) codes via Progressive-Edge Growth (PEG) [3] were explored in [2]. PEG works iteratively per columns, adding a fixed number of non-zero elements at the locations which locally maximize the girth of the associated Tanner graph. However, a sequence of locally optimal decisions may not lead to a global minimum and $\mu < 1$ cannot always be guaranteed. Recently, Gupta [4] and Barragan [5] proposed a family of novel functions built upon Hamiltonian cycles on hypercube graphs, similarly to Gray codes. In this work, we propose a practical methodology which allows for $\gamma_{\text{SR}} > 1$, and ensures good recoverability properties for $\eta \ll 1$. In contrast to [4, 5], our methodology is built upon low-density codes, as they also minimize the integration of background light, and allow for a faster computation if a sparsity-oriented programming is adopted.

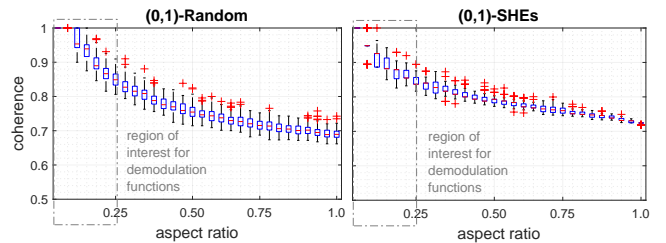


Fig. 2. Coherence vs aspect ratio of sensing matrices generated via random (0,1)-binary codes (left) and Scrambled Hadamard Ensembles (SHEs) with (0,1)-rescaling (right) over $n_{\text{real}} = 100$ realizations.

II. METHODOLOGY

The proposed coding scheme, called gradient-Combinatorial (GComb) [2], iteratively adds $[\vec{a}^j]_{j=1}^n$, and consists of the following steps:

- 1) We select the location of the n_{deg} non-zero elements in each of the n columns from their possible combinations without repetition in the m rows. This ensures $\mu < 1$ in the (0,1)-binary codes that the demodulation functions are built upon.
- 2) In real operation, the non-zero transition time of binary control signals yields coincidences of rising and falling edges. This

may lead to identical columns far apart from each other in \mathbf{A} . We include an evaluation step when adding a new element to \mathbf{A} . Firstly, we generate a new matrix \mathbf{A}_{dif} , given by the differences between the elements of adjacent columns, and evaluate its coherence (μ_{dif}). If the added non-zero element yields $\mu_{\text{dif}} = 1$, we remove it from the set of candidates. This evaluation step translates into a deterministic arrangement of $[\vec{a}^j]_{j=1}^n$, and can be applied to any other methodology such as LDPC-PEG [2].

GComb yields an upper bound for γ_{SR} such that $\mu < 1$. We push this limit further by introducing near-to-optimal on-grid offsets (implemented through time delays) between $[\vec{a}_i]_{i=1}^m$. In our methodology [6], given \mathbf{A} , we sequentially work per rows, evaluate the impact of any possible on-grid offset, and select the one which maximizes the minimum inter-column distance. Our technique allows for a reduction of the number of highly-correlated columns, and outperforms other methodologies such as the ones based on uniform or random on-grid offsets. Fig. 3 presents a comparison of the distributions of $n_{\text{samples}} = 42$ samples (columns of \mathbf{A}) in the \mathbb{R}^3 hyper-sphere [6]. We observe an increase of the chordal distance between adjacent samples when the shifts are implemented, which yields a reduction of μ .

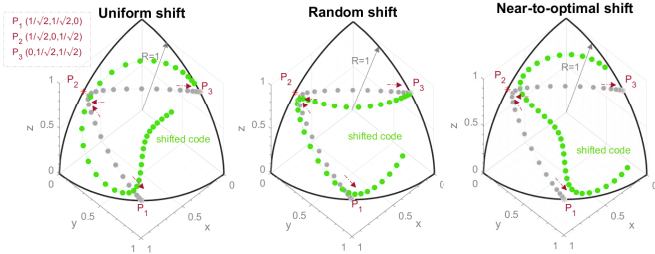


Fig. 3. Representation of normalized columns of the sensing matrices on the unit hyper-sphere on \mathbb{R}^3 for $n_{\text{steps}} = 14$, and $n_{\text{deg}} = 2$ when implementing uniform (left), random (center), and near-to-optimal (right) on-grid shifts [6].

III. NUMERICAL SIMULATIONS

At ZESS, we have designed a rotary PB-ToF camera that allows us to implement the presented computational sensing approaches to bring long-range wide-area ToF imaging to a new level of accuracy [2]. The design parameters of our prototype used in this numerical simulation are shown in Table I.

TABLE I
DESIGN PARAMETERS OF OUR TOF CAMERA

Operational parameter	Acronym	Value
Modulation frequency (element bandwidth)	f_m	448 MHz
Repetition frequency	f_r	3.5 MHz
Number of sub-steps for super-resolution	n_{steps}	8
Cross-correlation function	FWHM	0.4 ns
Number of measurements	m	14
Number of non-zero elements per column	n_{deg}	3

Fig.4 shows the sensing matrices (left), the corresponding normalized Gram matrices (center), and the histograms of column cross-correlations (right) using random (0,1)-binary codes, (0,1)-Scrambled Hadamard Ensembles (SHEs), GComb, and GComb followed by the implementation of near-to-optimal on-grid shifts. We observe a drastic reduction of the number of highly-correlated columns, and a concentration of them in a narrow region close to the diagonal of the normalized Gram matrix for GComb. In addition, we identify a further reduction of the number of highly-correlated columns when introducing near-to-optimal shifts in a matrix built via GComb.

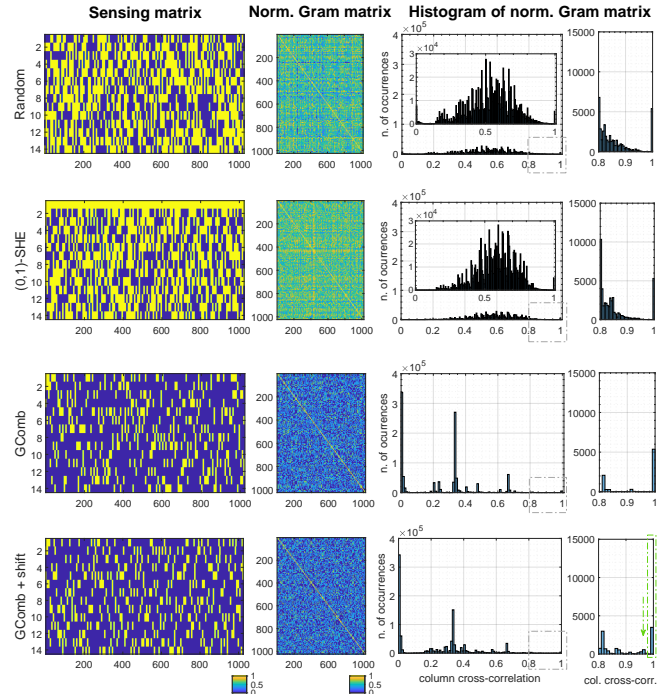


Fig. 4. Sensing matrices, normalized Gram matrices and histograms of column cross-correlations generated via random (0,1)-binary codes, Scrambled Hadamard Ensembles with (0,1)-rescaling, gradient-Combinatorial, and gradient-Combinatorial + near-to-optimal shifts.

IV. CONCLUSION

In this paper, we have presented a practical methodology for the generation of sensing matrices that makes use of low-density codes and ensures good coherence properties for very low aspect ratios. This allows for the use of these codes in close to real-time PB-ToF systems working with coded modulation/demodulation schemes. Prospective work includes the implementation and evaluation of such schemes in our prototype during real operation.

REFERENCES

- [1] A. Bhandari, M. Heredia Conde, and O. Loffeld, "One-bit time-resolved imaging," *IEEE Transactions on Pattern Analysis and Machine Intelligence*, vol. 42, no. 7, pp. 1630–1641, 2020.
- [2] A. Lopez Paredes, M. Heredia Conde, and O. Loffeld, "Sparsity-aware 3D ToF sensing," *IEEE Sensors Journal*, vol. 23, no. 4, pp. 1–1, 2023.
- [3] G. Sriruchataboob, A. Bajpai, L. Wuttisittikul, and P. Kovintavewat, "PEG-like algorithm for LDPC codes," in *2014 International Electrical Engineering Congress (iEECON)*, 2014, pp. 1–4.
- [4] M. Gupta, A. Velten, S. K. Nayar, and E. Breitbach, "What are optimal coding functions for Time-of-Flight imaging?" *ACM Trans. Graph.*, vol. 37, no. 2, Feb. 2018.
- [5] F. Gutierrez-Barragan, S. A. Reza, A. Velten, and M. Gupta, "Practical coding function design for Time-Of-Flight imaging," in *IEEE Conference on Computer Vision and Pattern Recognition, CVPR 2019, Long Beach, CA, USA, June 16-20, 2019*. Computer Vision Foundation / IEEE, 2019, pp. 1566–1574.
- [6] A. Lopez Paredes, M. Heredia Conde, and O. Loffeld, "CS-ToF sensing by means of greedy bi-lateral fusion and near-to-optimal low-density codes," in *2022 30th European Signal Processing Conference (EUSIPCO)*, 2022.